Electronic Supplementary Information for Dalton Transactions
This journal is © The Royal Society of Chemistry 2010

Supporting information

Self-assembly of silver (I) metallomacrocycles using unsupported 1,4-substituted-1,2,3-triazole "Click" ligands.

Martin L.Gower and James D Crowley.*

Department of Chemistry, University of Otago, PO Box 56, Dunedin, New Zealand

jcrowley@chemistry.otago.ac.nz

This journal is © The Royal Society of Chemistry 2010

Table of Contents **S2**

1. ^{1}H NMR Spectra of synthesized compounds. **S4**

^{1}H NMR (d_6-acetone, 300K) of **2a**. **S4**

^{1}H NMR (d_6-acetone, 300K) of **2b**. **S5**

^{1}H NMR (d_6-acetone, 300K) of **3a**. **S6**

^{1}H NMR (d_6-acetone, 300K) of **3b**. **S7**

^{1}H NMR (d_6-acetone, 300K) of **4a**. **S8**

Figure 1. Partial ^{1}H NMR spectra (300 MHz, d_6-acetone, 300 K) of a) Ligand **2a**, b) $[Ag_2(\mathbf{2a})_2](SbF_6)_2$, **4a**. **S8**

^{1}H NMR (d_6-acetone, 300K) of **4b**. **S9**

Figure 2. Partial ^{1}H NMR spectra (300 MHz, d_6-acetone, 300 K) of a) Ligand **2b**, b) $[Ag_2(\mathbf{2b})_2](SbF_6)_2$. **S9**

^{1}H NMR (d_6-acetone, 300K) of **5a**. **S10**

Figure 3. Partial ^{1}H NMR spectra (300 MHz, d_6-acetone, 300 K) of a) Ligand **3a**, b) $[Ag_2(\mathbf{3a})_2](SbF_6)_2$, **5a**. **S10**

^{1}H NMR (d_6-acetone, 300K) of $[Ag_2(\mathbf{5b})_2](SbF_6)_2$. **S11**

Figure 4. Partial ^{1}H NMR spectra (300 MHz, d_6-acetone, 300 K) of a) Ligand **3b**, b) $[Ag_2(\mathbf{3b})_2](SbF_6)_2$, **5b**. **S11**

2. SPARTAN CPK models of the silver(I) complexes. **S12**

Figure 5. Space Filling (CPK, left) and tube (right) molecular models of the trimeric 3:3 complex formed between **2a** and $Ag(SbF_6)$. **S12**

Figure 6. Space Filling (CPK, left) and tube (right) molecular models showing the complex formed if Ag(I) binding to the ligands (**3a** and 3**b**) was through the N2 nitrogen of the triazole. **S12**

3. HR-ESMS Spectra of the silver complexes. **S13**

Figure 7. HR-ESMS (CH_3CN) of $[Ag_2(\mathbf{2a})_2](SbF_6)_2$, **4a**. **S13**

Figure 8. Observed and Calculated isotopic distributions for the $[Ag_2(\mathbf{2a})_2](SbF_6)^+$ ion. **S14**

Figure 9. HR-ESMS (CH_3CN) of $[Ag_2(\mathbf{2b})_2](SbF_6)_2$, **4b**. **S15**

Figure 10. Observed and Calculated isotopic distributions for the $[Ag_2(\mathbf{2b})_2](SbF_6)_2^+$ ion. **S16**

Figure 11. HR-ESMS (CH_3CN) of $[Ag_2(\mathbf{3a})_2](SbF_6)_2$, **5a**. **S17**

Figure 12. Observed and Calculated isotopic distributions for the $[Ag_2(\mathbf{3a})_2](SbF_6)_2^+$ ion. **S18**

Figure 13. HR-ESMS (CH_3CN) of $[Ag_2(\mathbf{3b})_2](SbF_6)_2$, **5b**. **S19**

Figure 15. Observed and Calculated isotopic distributions for the $[Ag_2(\mathbf{3b})_2](SbF_6)_2^+$ ion. **S20**

4. X-ray Crystallographic Data **S21**

Figure 15. ORTEP (top) and space filling (bottom) views of the $[\mathbf{2a}_2Ag_2]^{2+}$ cation. **S21**

Figure 16. Two views of $[(\mathbf{2a})_2Ag_2](SbF_6)_2$ **(3a)** showing the close contacts between the SbF_6^- anions and the Ag(I) ions. **S22**

Figure 17. Two views of the extended structure of $[(\mathbf{2a})_2Ag_2](SbF_6)_2$ **(3a).** a) a ball and stick diagram and b) a space filing diagram. **S22**

Figure 18. ORTEP (top) and space filling (bottom) views of the $[(\mathbf{2b})_4Ag_2]^{2+}$ cation. **S23**

Figure 19. Two views of the extended structure of $[(\mathbf{2b})_2Ag_2](SbF_6)_2$ **(3b).** a) a ball and stick diagram and b) a space filing diagram. **S24**

Figure 20. An ORTEP diagram of the $[(\mathbf{3b})_4Ag_2]^{2+}$ cation. **S24**

Figure 21. Two views of the complete cationic unit of $[(\mathbf{3b})_2Ag_2](SbF_6)_2$ **(5b).** a) a ball and stick diagram and b) a space filing diagram. **S25**

Figure 22. Two views of the extended structure of $[(\mathbf{3b})_2Ag_2](SbF_6)_2$ **(5b).** a) a ball and stick diagram and b) a space filing diagram. **S25**

4.1 X-Ray data collection and refinement for 5b (acetone). **S26**

Table 1 Crystal data and structure refinement for **5b** (acetone)**.** **S26**

Figure 23. An ORTEP diagram of $[(\mathbf{3b})_4Ag_2]^{2+}$ cation from the of the crystal structure **5b** (acetone) **S27**

5. References. **S27**

1. ^{1}H NMR spectra of synthesized compounds.

^{1}H NMR (d_6-acetone, 300K) of **2a**.

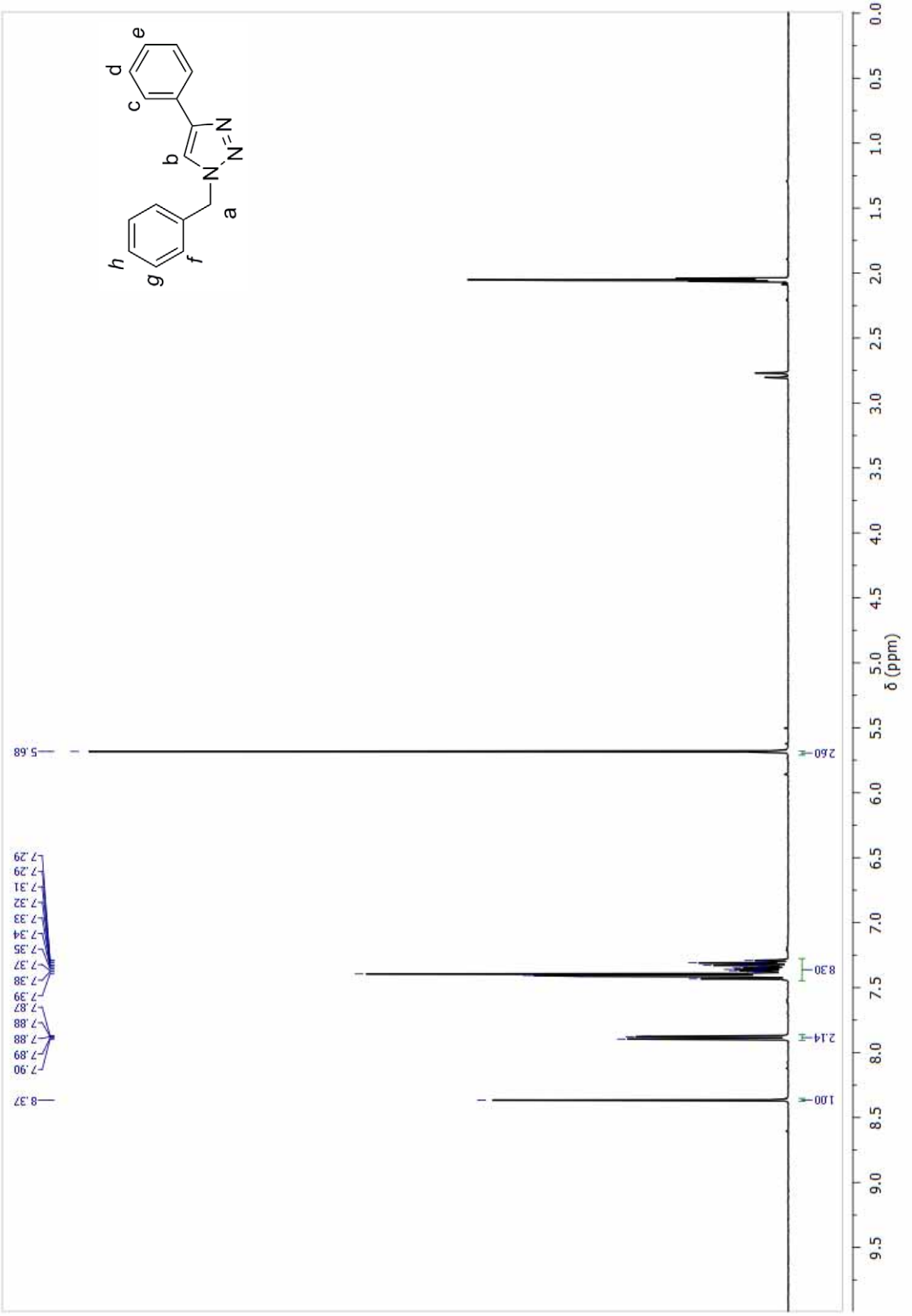

^{1}H NMR (d_6-acetone, 300K) of **2b**.

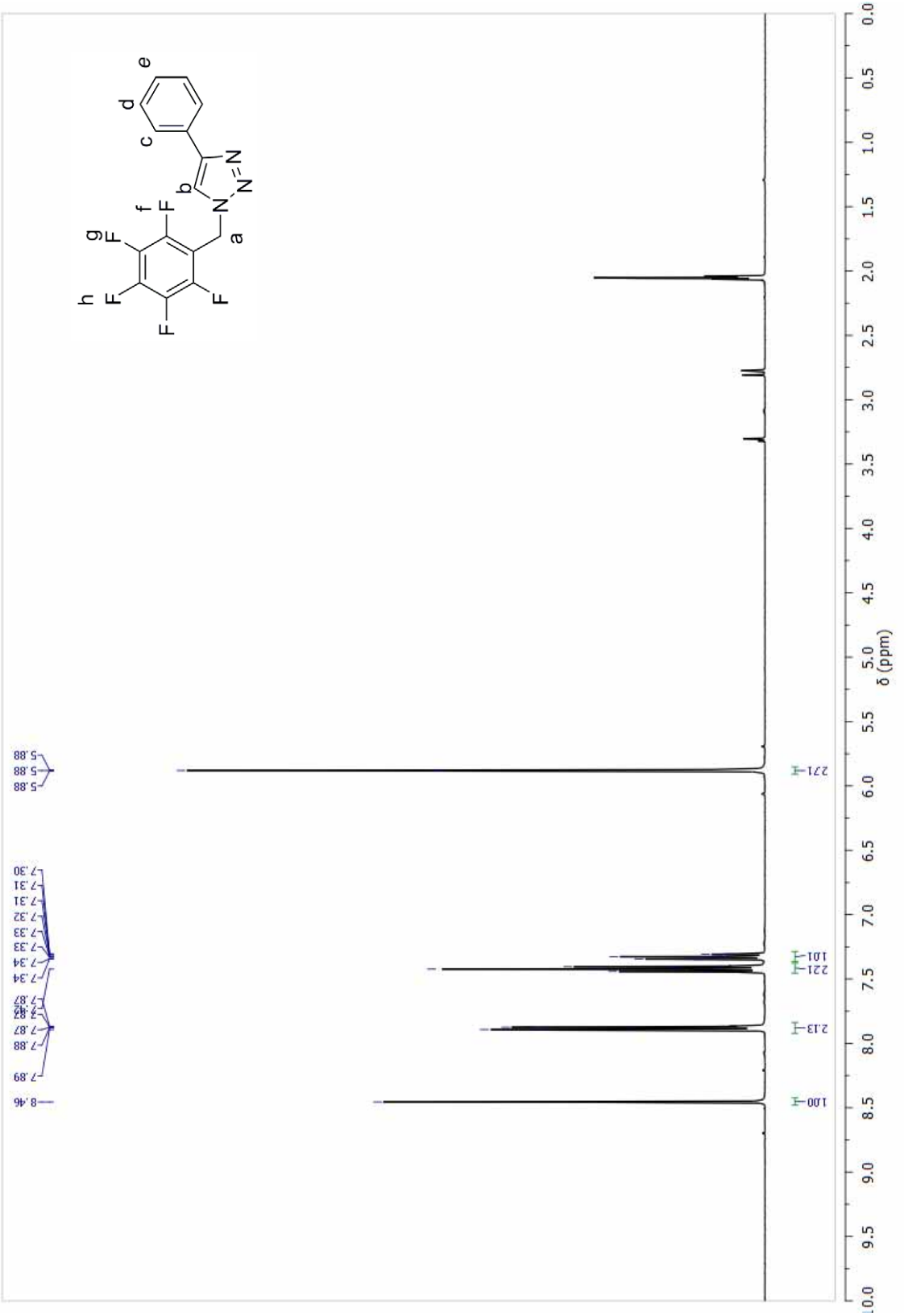

^{1}H NMR (d_6-acetone, 300K) of **3a**.

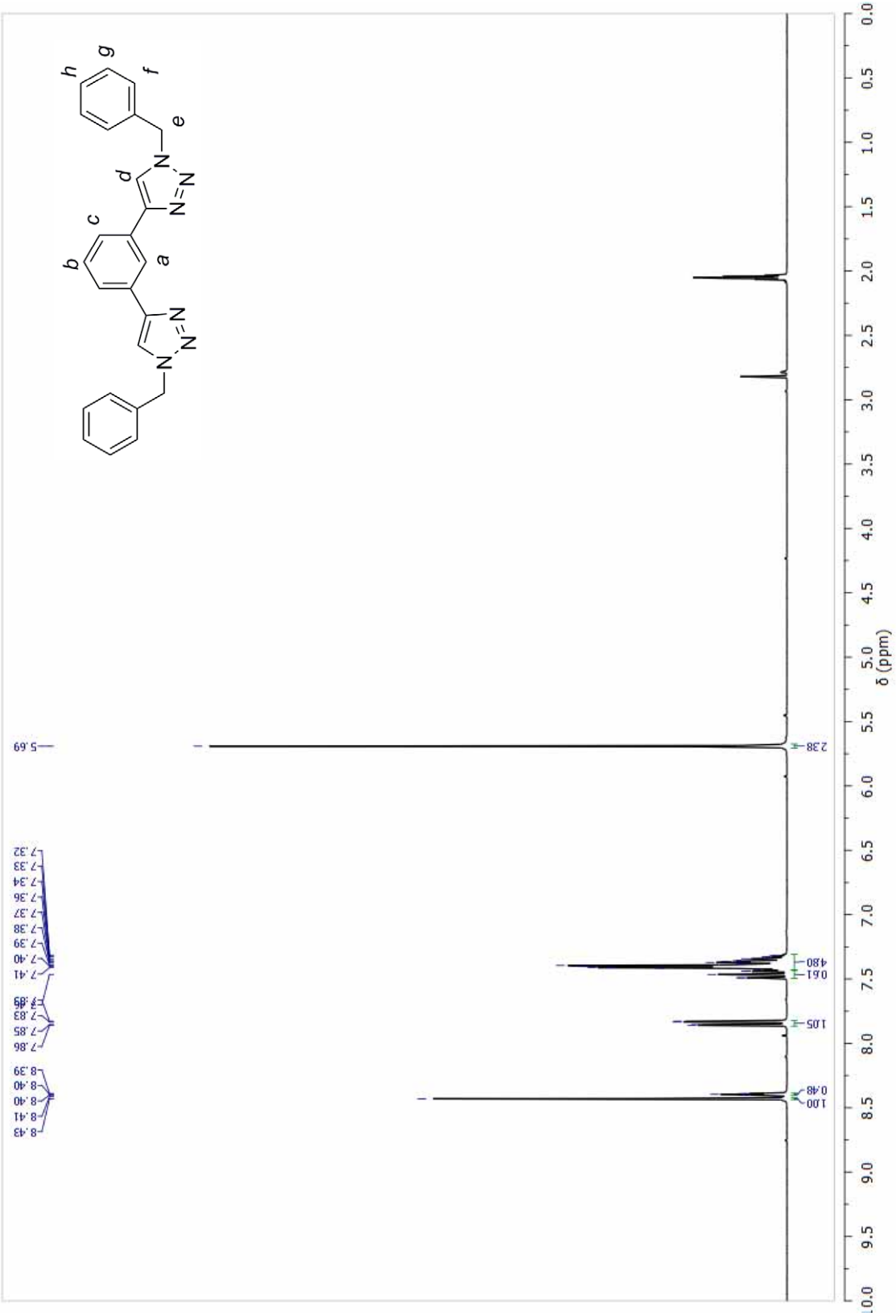

^{1}H NMR (d_6-acetone, 300K) of **3b**.

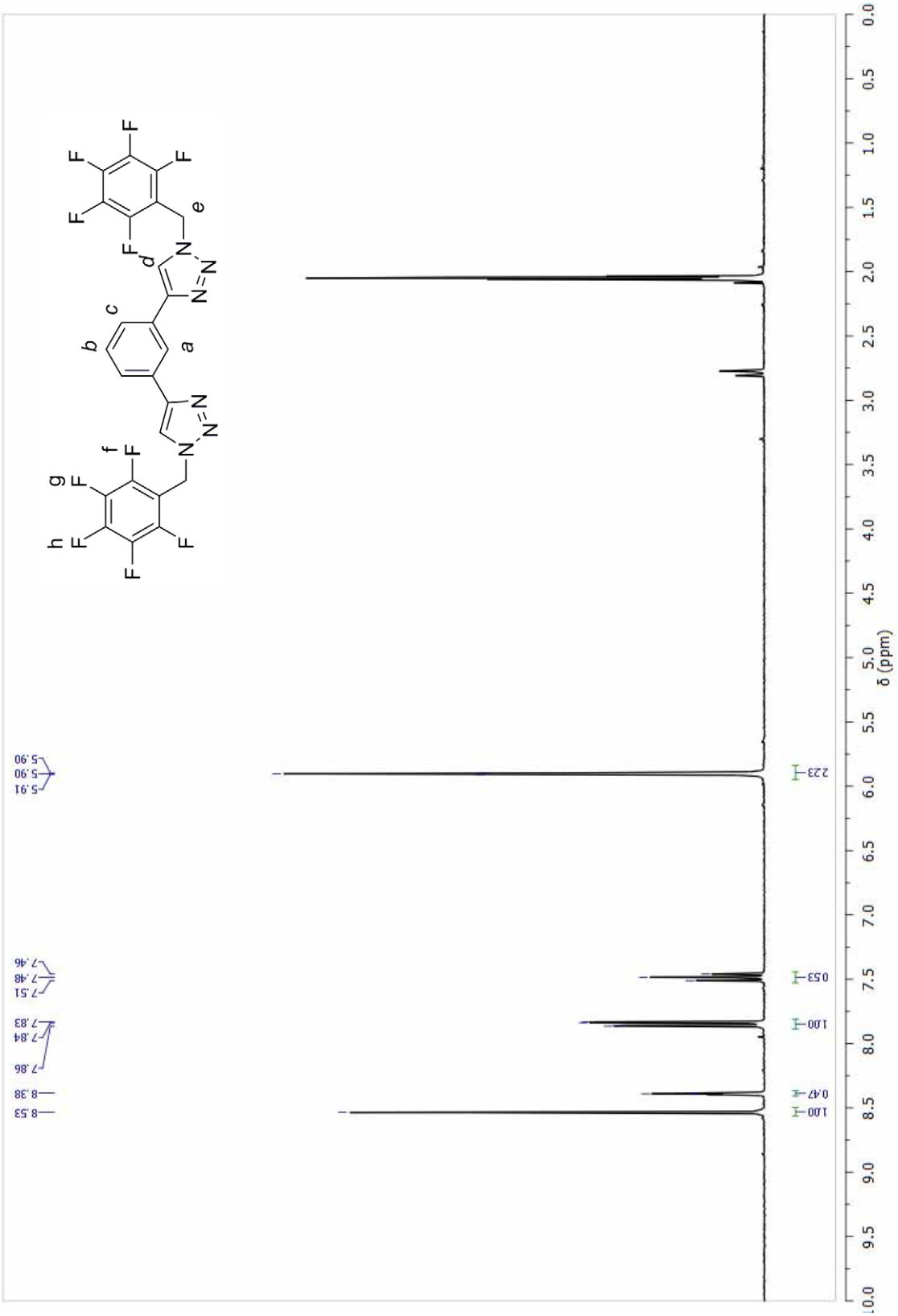

4.1 ^{1}H NMR spectra of the silver(I) complexes.

^{1}H NMR (d_6-acetone, 300K) of **4a**.

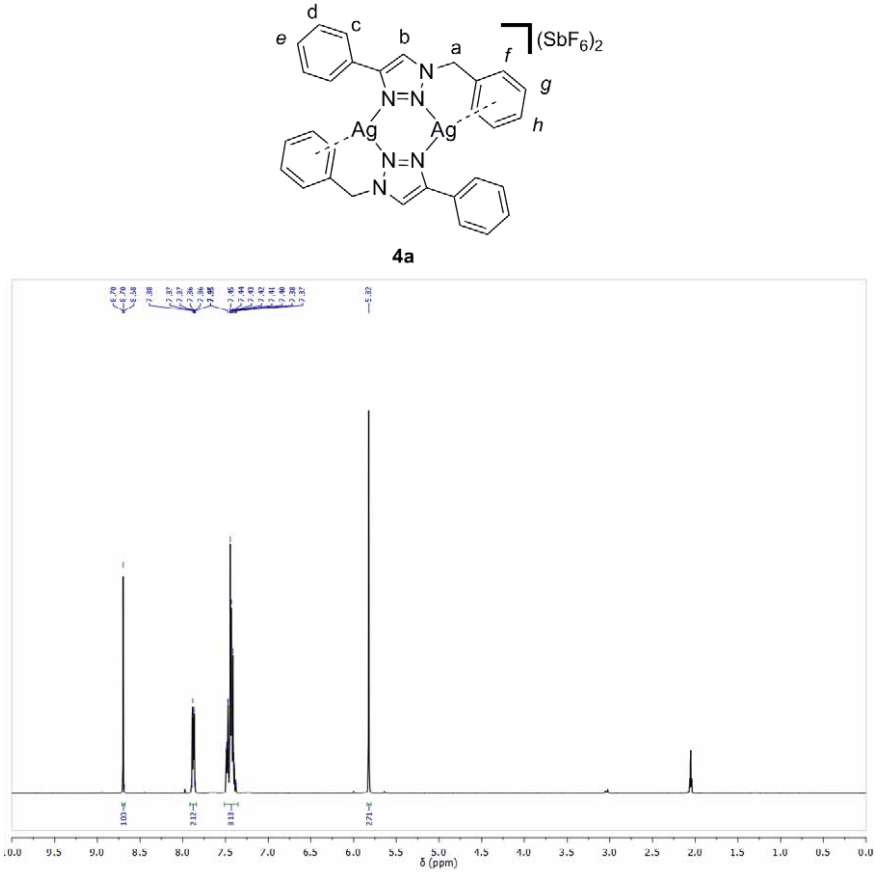

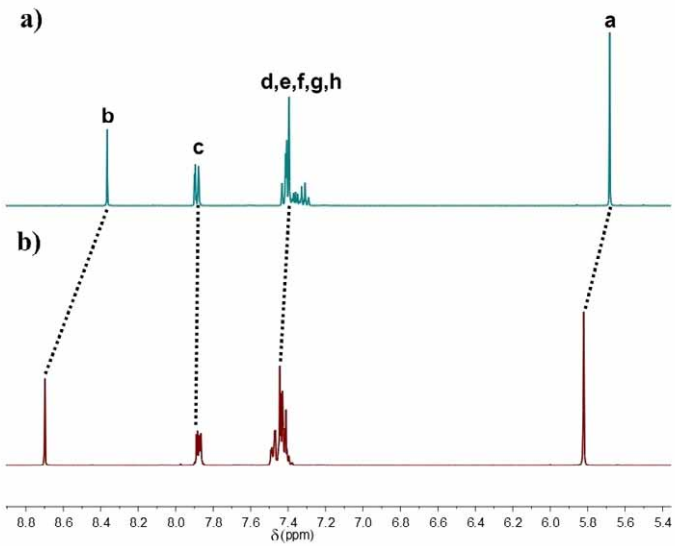

Figure 1. Partial ^{1}H NMR spectra (300 MHz, d_6-acetone, 300 K) of a) Ligand **2a**, b) silver complex **4a**.

^{1}H NMR (d_6-acetone, 300K) of **4b**.

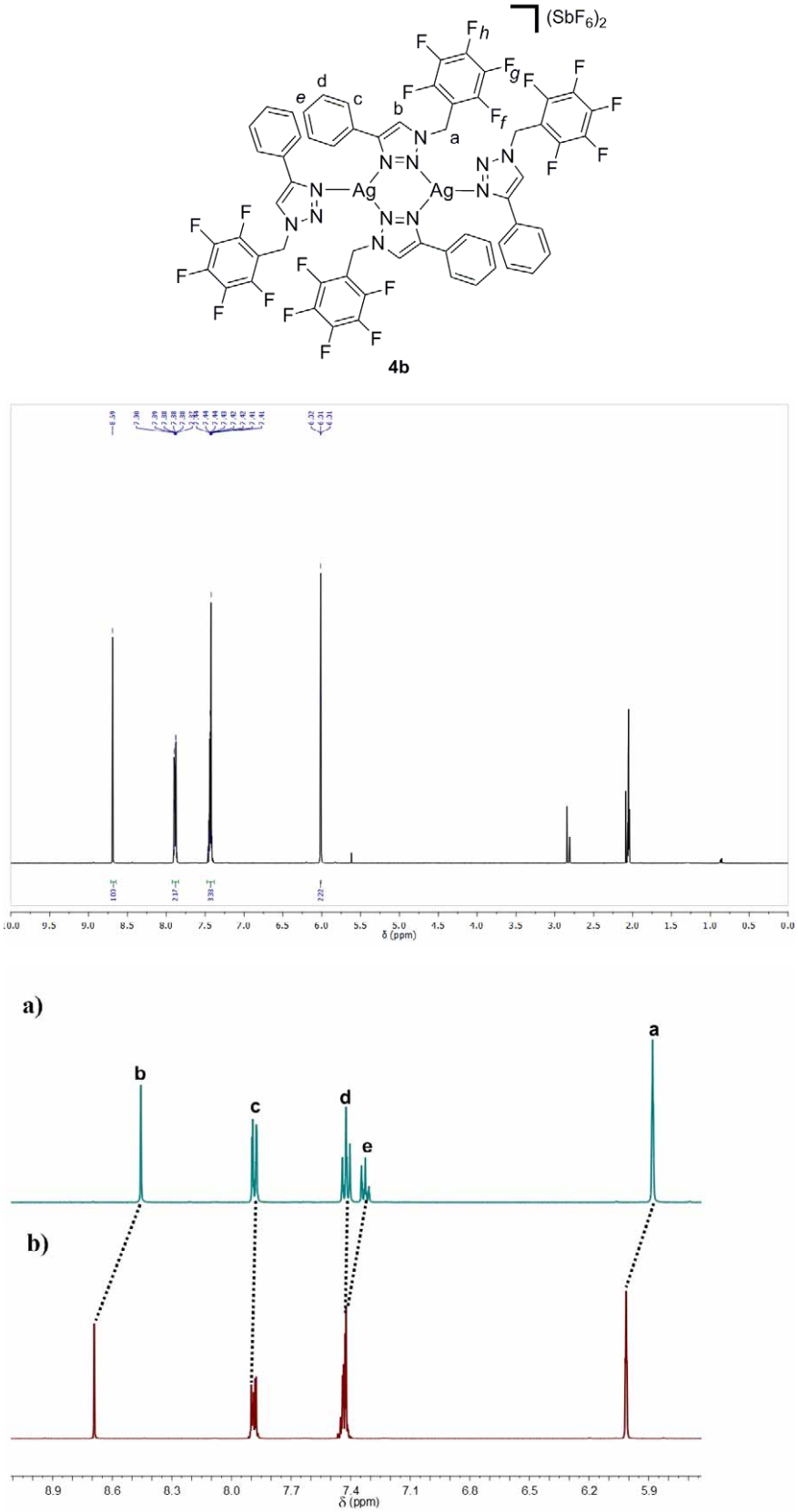

Figure 2. Partial ^{1}H NMR spectra (300 MHz, d_6-acetone, 300 K) of a) Ligand **2b**, b) silver complex **4b**.

^{1}H NMR (d_6-acetone, 300K) of **5a**.

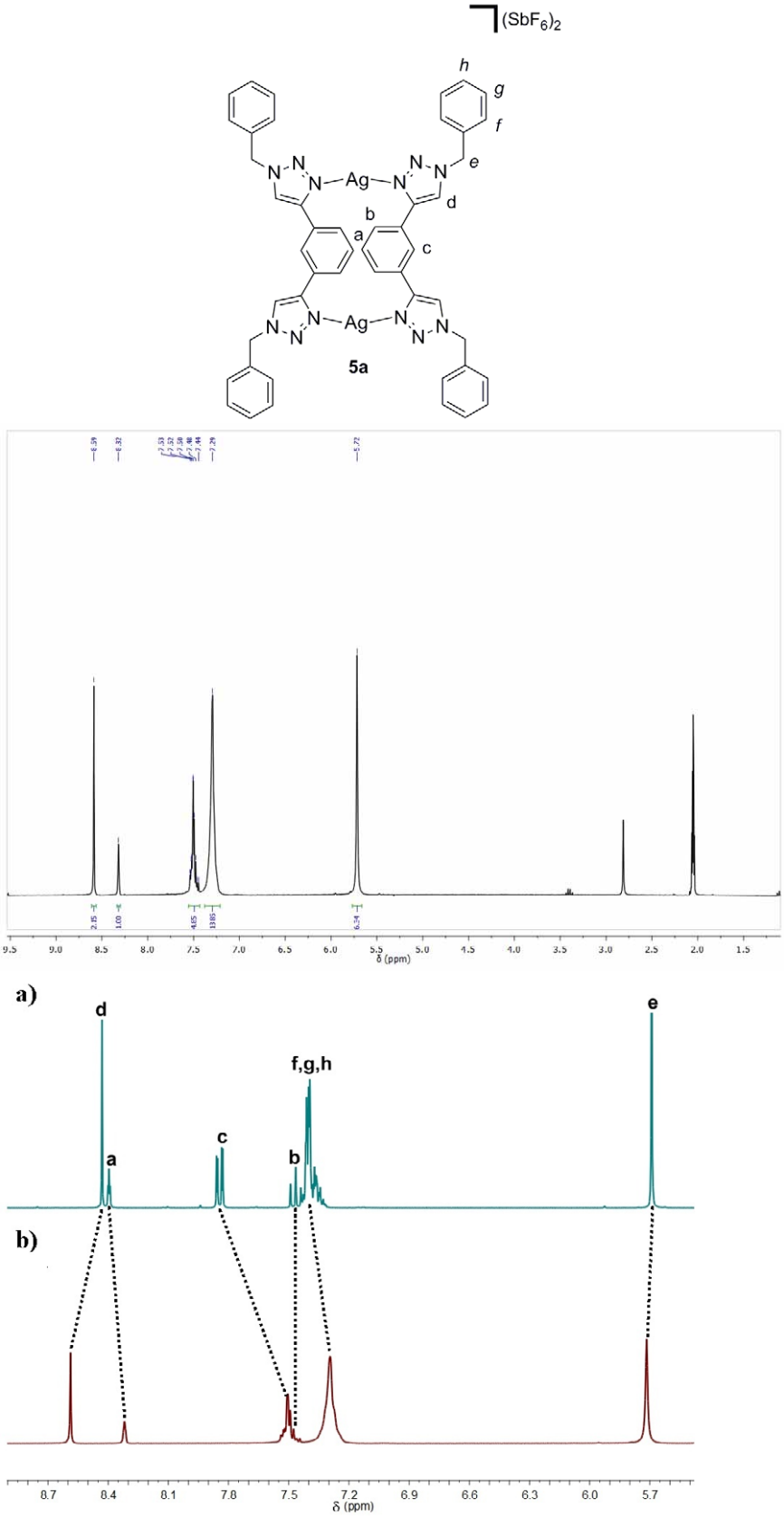

Figure 3. Partial ^{1}H NMR spectra (300 MHz, d_6-acetone, 300 K) of a) Ligand **3a**, b) silver complex **5a**.

^{1}H NMR (d_6-acetone, 300K) of **5b**.

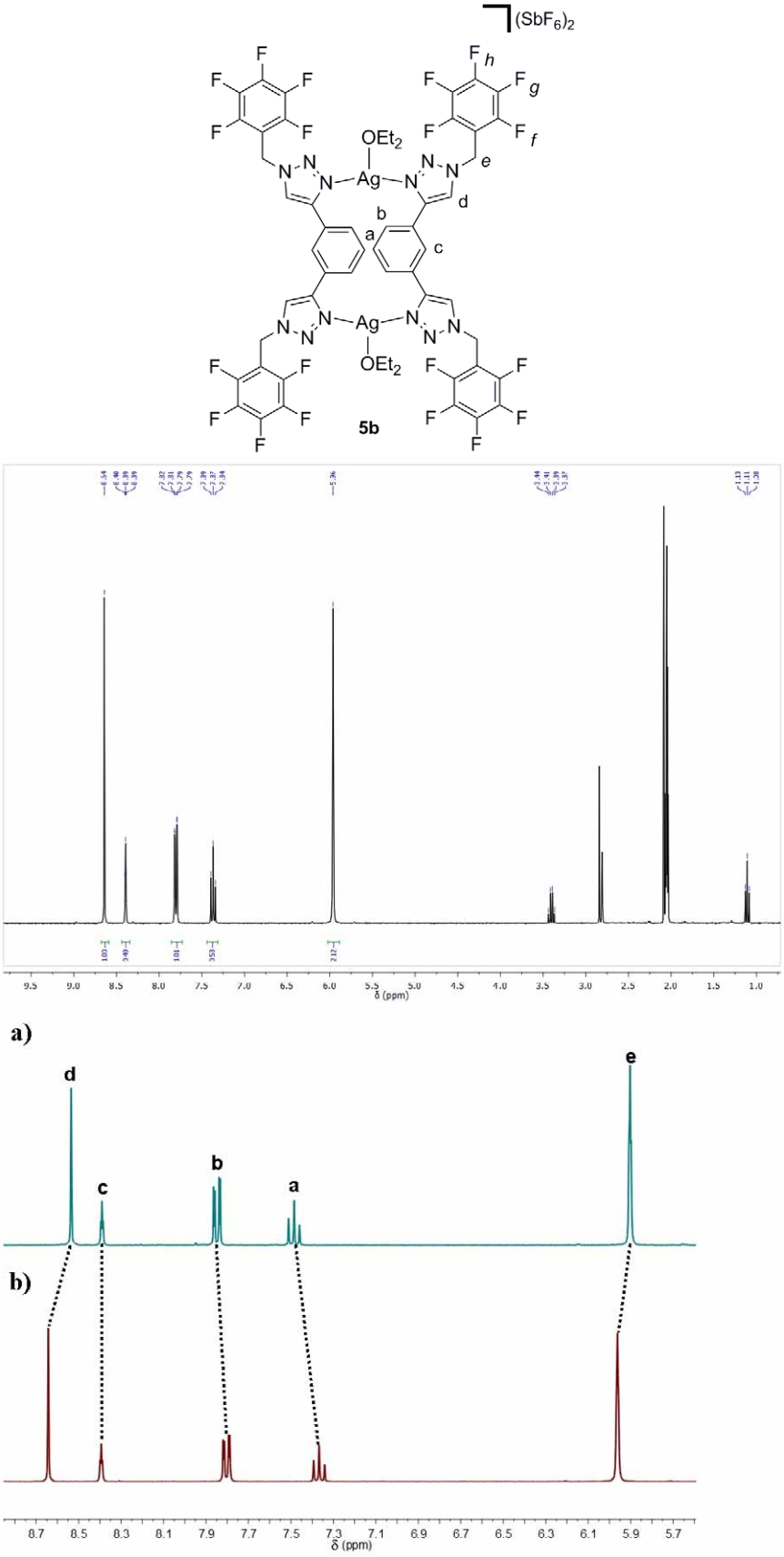

Figure 4. Partial ^{1}H NMR spectra (300 MHz, d_6-acetone, 300 K) of a) Ligand **3b**, b) **5b**.

2. SPARTAN CPK molecular models of the complexes.

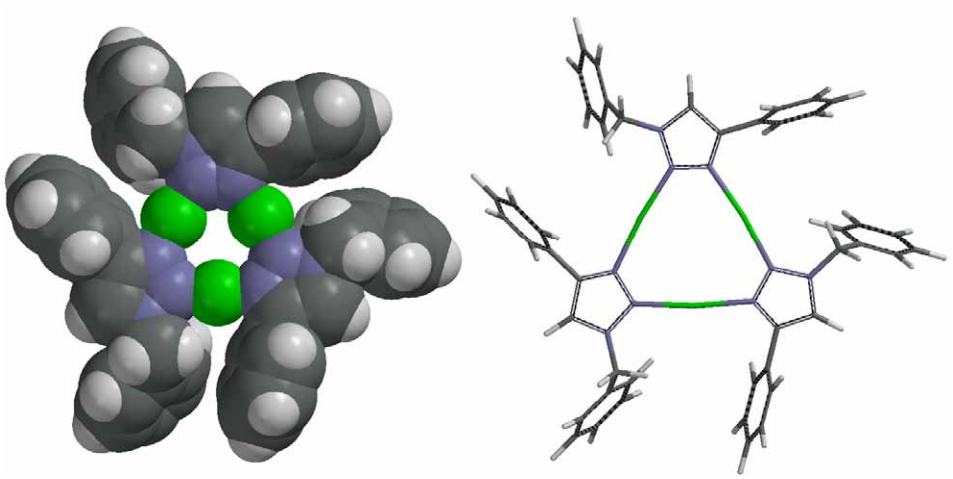

Figure 5. Space Filling (CPK, left) and tube (right) molecular models of the trimeric 3:3 complex formed between **2a** and $Ag(SbF_6)$. (Spartan '06 Essential Edition for Windows, Wavefunction, Irvine, CA)

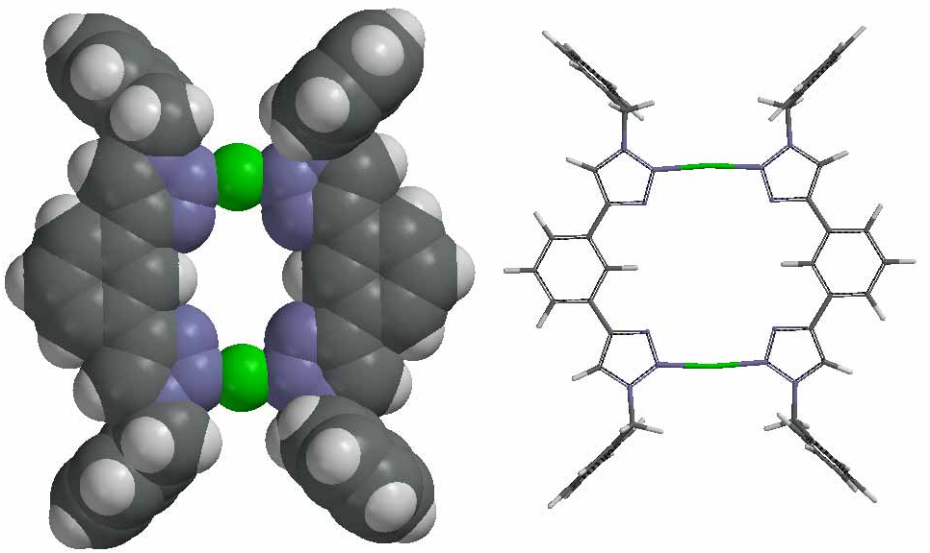

Figure 6. Space Filling (CPK, left) and tube (right) molecular models showing the complex formed if Ag(I) binding to the ligands (**3a** and **3b**) was through the N2 nitrogen of the triazole. (Spartan '06 Essential Edition for Windows, Wavefunction, Irvine, CA)

3. HR-ESMS spectra of the silver(I) complexes.

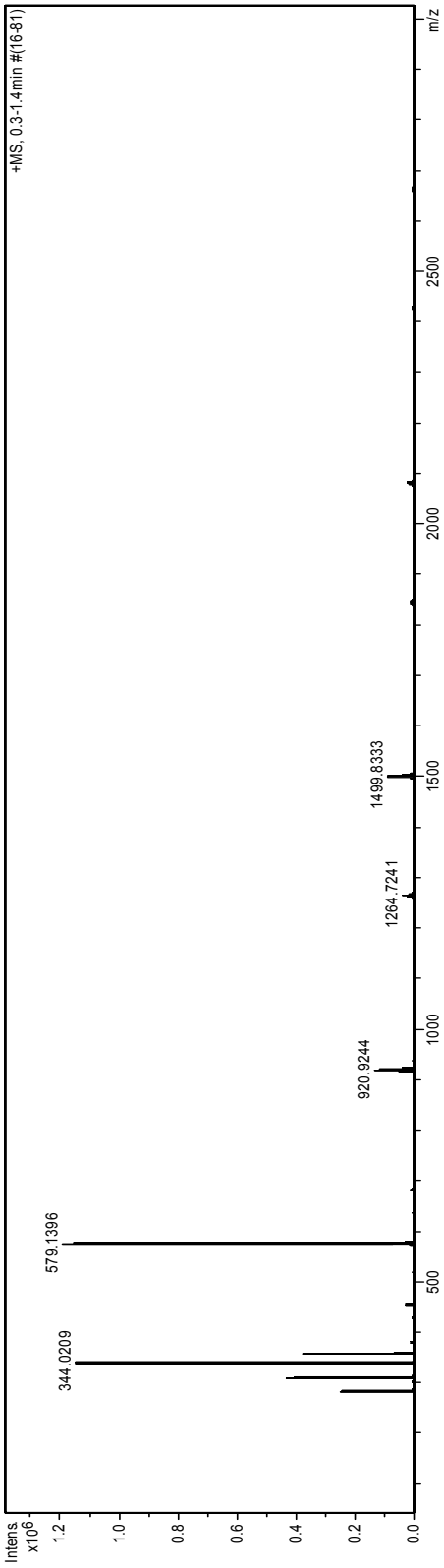

Figure 7. HR-ESMS (CH_3CN) of $[Ag_2(\mathbf{2a})_2](SbF_6)_2$, **4a**: *m/z* = 344.0209 $[Ag(\mathbf{2a})]^+$ (calc. for $C_{15}H_{13}AgN_3$ 344.0157), 579.1396 $[Ag(\mathbf{2a})_2]^+$ (calc. for $C_{30}H_{26}AgN_6$ 579.1267), 920.9243 $[Ag_2(\mathbf{2a})_2](SbF_6)^+$ (calc. for $C_{30}H_{26}Ag_2F_6N_6Sb$ 920.9245), 1499.8332 $[Ag_3(\mathbf{2a})_3](SbF_6)_2^+$ (calc. for

$C_{45}H_{39}Ag_3F_{12}N_9Sb_2$ 1499.8367).

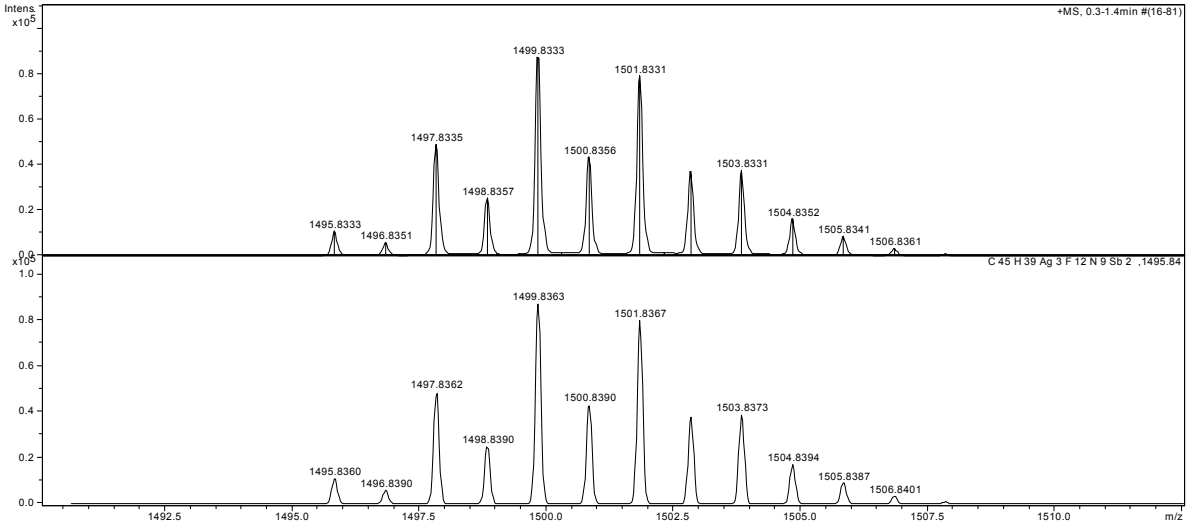

Figure 8. Observed (top) and calculated (bottom) isotopic distribution for the $[Ag_3(\mathbf{2a})_3](SbF_6)_2^+$ ion.

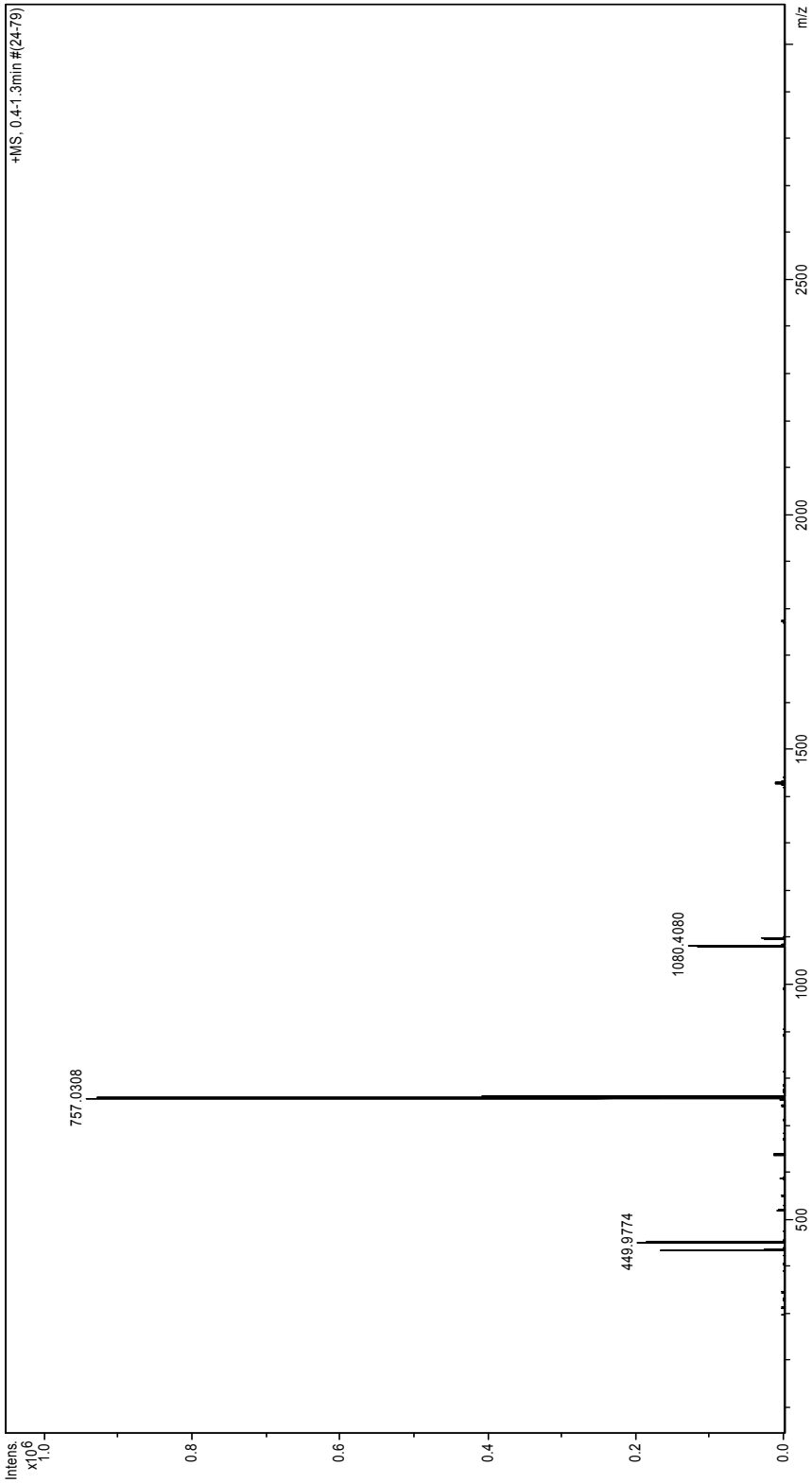

Figure 9. HR-ESMS (CH_3CN) of $[Ag_2(\mathbf{2b})_2](SbF_6)_2$, **4b:** *m/z* = 449.9775 $[Ag(\mathbf{2b})H_2O]^+$ (calc. for $C_{15}H_{10}AgF_5N_3O$ 449.9795), 757.0273 $[Ag(\mathbf{2b})_2]^+$ (calc. for $C_{30}H_{16}AgF_{10}N_6$ 757.0328), 1425.8874 $[Ag_2(\mathbf{2b})_3](SbF_6)^+$ (calc. for $C_{45}H_{24}Ag_2F_{21}N_9Sb$ 1425.8960), 1769.6885 $[Ag_3(\mathbf{2b})_3](SbF_6)^+$ (calc. for

$C_{45}H_{24}Ag_3F_{27}N_9Sb_2$ 1769.6953).

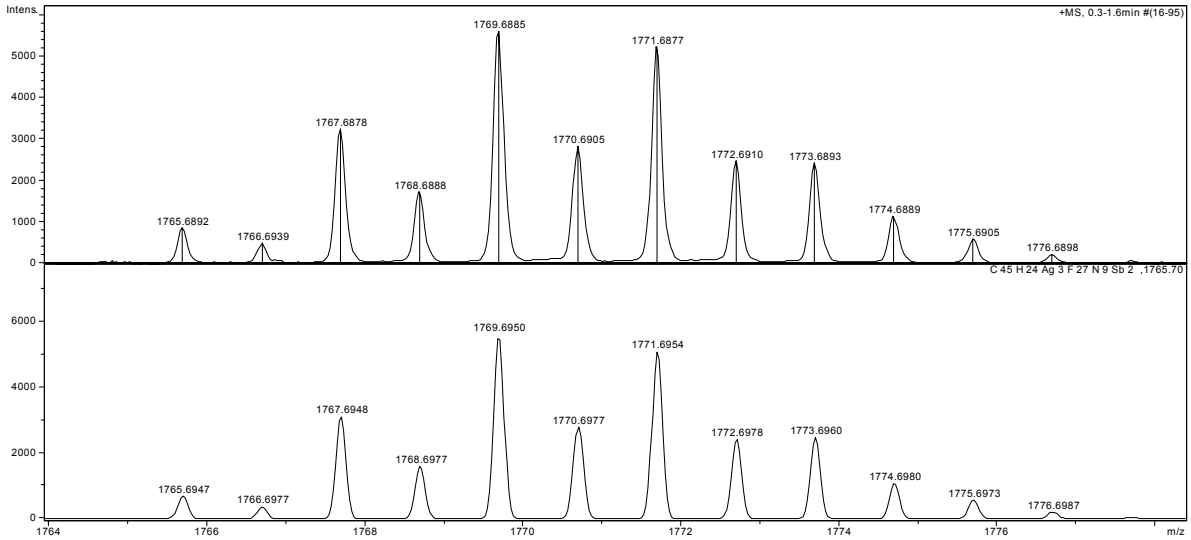

Figure 10. Observed (top) and calculated (bottom) isotopic distribution for the $[Ag_3(\mathbf{2b})_3](SbF_6)_2^+$ ion.

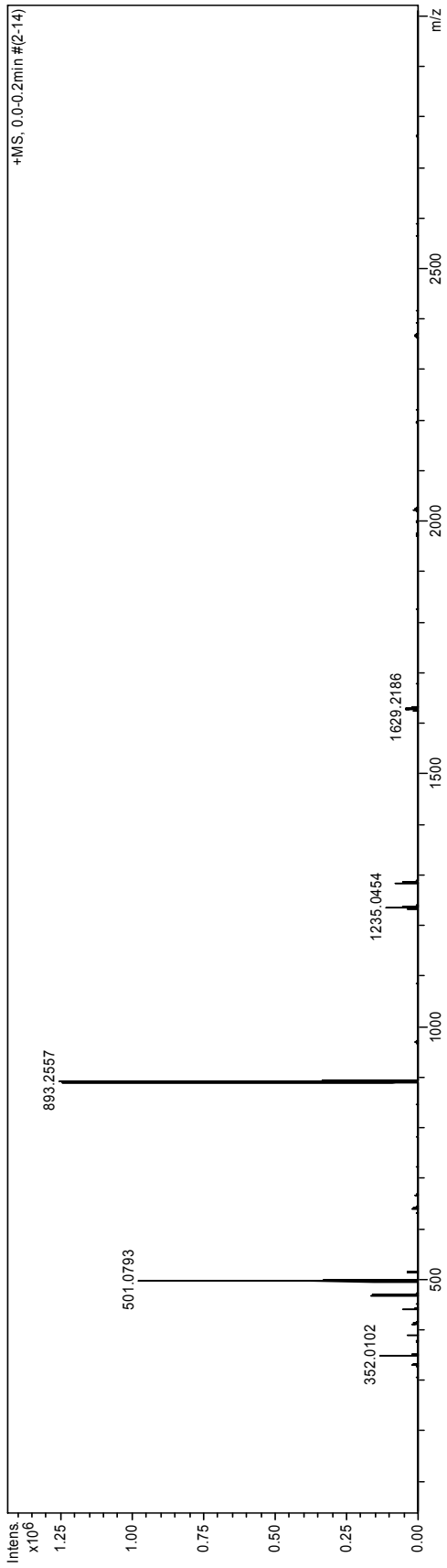

Figure 11. HR-ESMS (CH_3CN) of $[Ag_2(\mathbf{3a})_2](SbF_6)_2$, **5a**: *m/z* = 501.0789 $[Ag(\mathbf{3a})]^+$ (calc. for $C_{24}H_{20}N_6Ag$ 501.0797), 893.2551 $[Ag(\mathbf{3a})_2]^+$ (calc. for $C_{48}H_{40}AgN_6$ 893.2543), 1235.0454

$[Ag_2(\mathbf{3a})_2](SbF_6)^+$ (calc. for $C_{48}H_{40}N_{12}Ag_2SbF_6$ 1235.0540), 1629.2186 $[Ag_2(\mathbf{3a})_3](SbF_6)^+$ (calc. for $C_{72}H_{60}N_{18}Ag_2SbF_6$ 1629.2293).

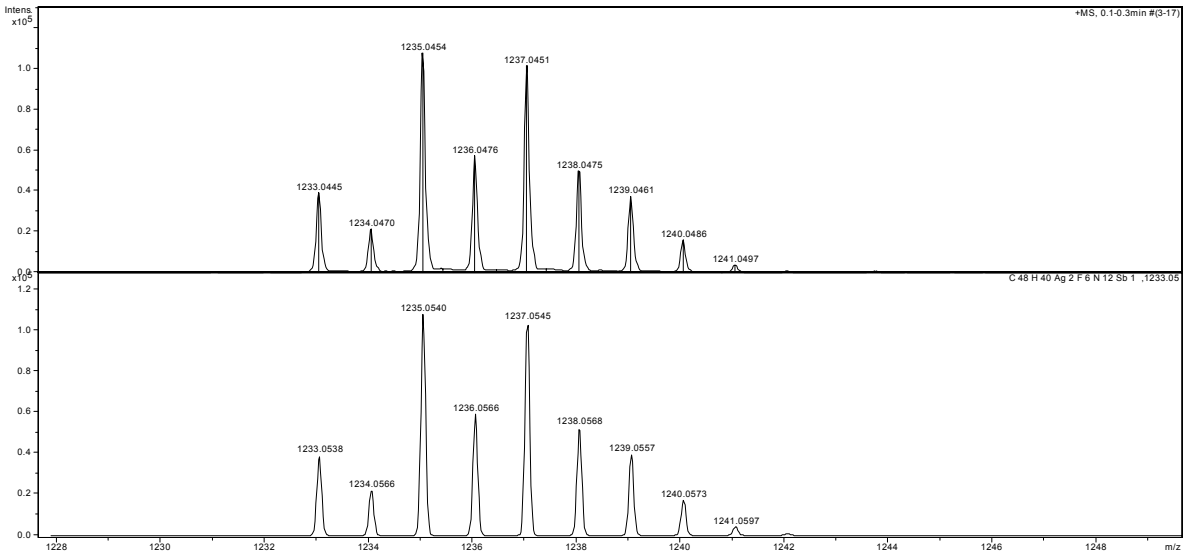

Figure 12. Observed (top) and calculated (bottom) isotopic distribution for the $[Ag_2(\mathbf{3a})_2](SbF_6)^+$ ion.

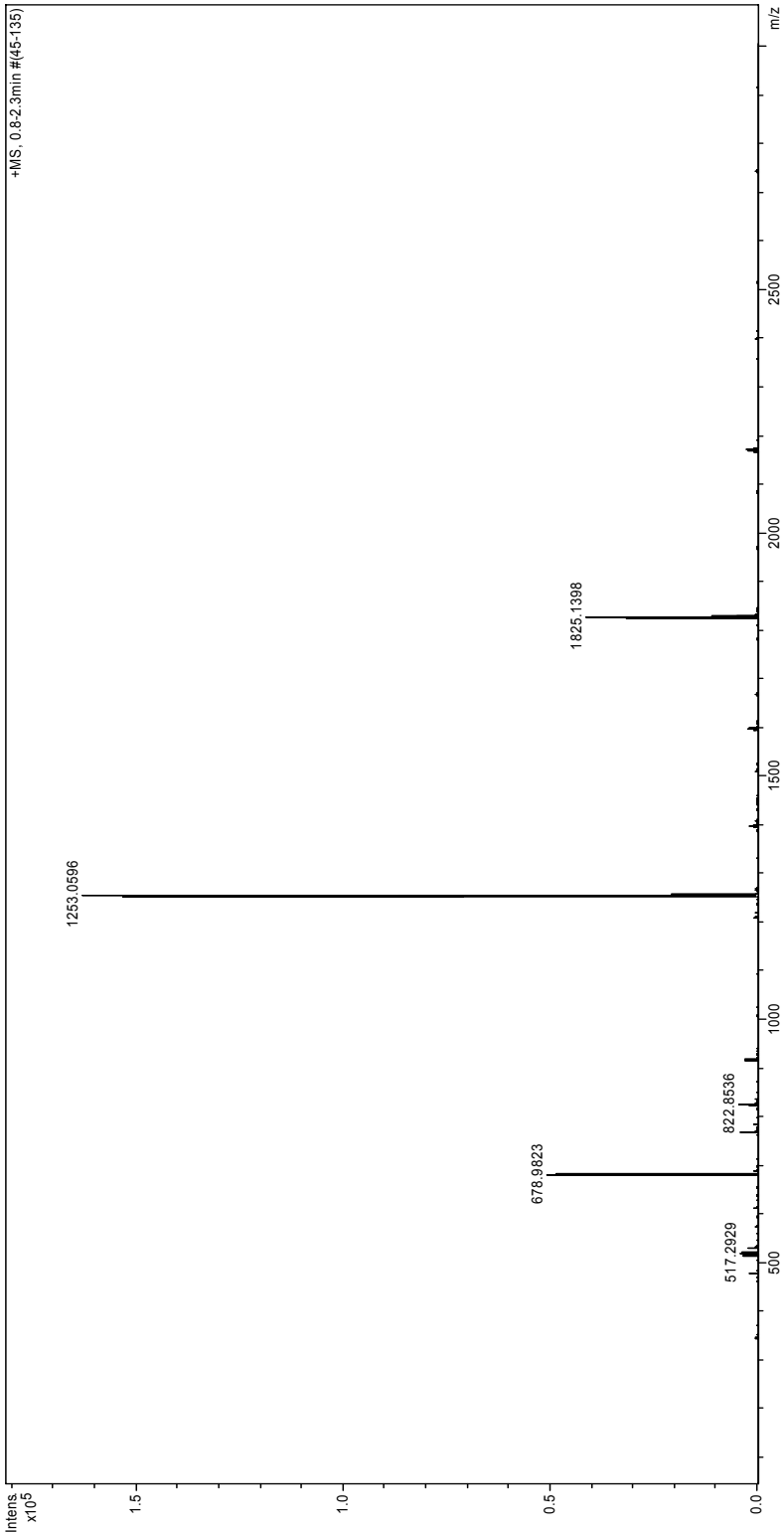

Figure 13. HR-ESMS (CH_3CN) of $[Ag_2(\mathbf{3b})_2](SbF_6)_2$, **5b**: m/z = 678.9967 $[Ag(\mathbf{3b})]^+$ (calc. for $C_{24}H_{10}AgF_{10}N_6$ 678.9858), 1253.0809 $[Ag(\mathbf{3b})_2]^+$ (calc. for $C_{48}H_{20}AgF_{20}N_{12}$ 1253.0662), 1594.8573

$[Ag_2(\mathbf{3b})_2](SbF_6)^+$ (calc. for $C_{48}H_{20}Ag_2F_{26}N_{12}Sb$ 1594.8655), 1825.1623 $[Ag(\mathbf{3b})_3]^+$ (calc. for $C_{72}H_{30}AgF_{30}N_{18}$ 1825.1469).

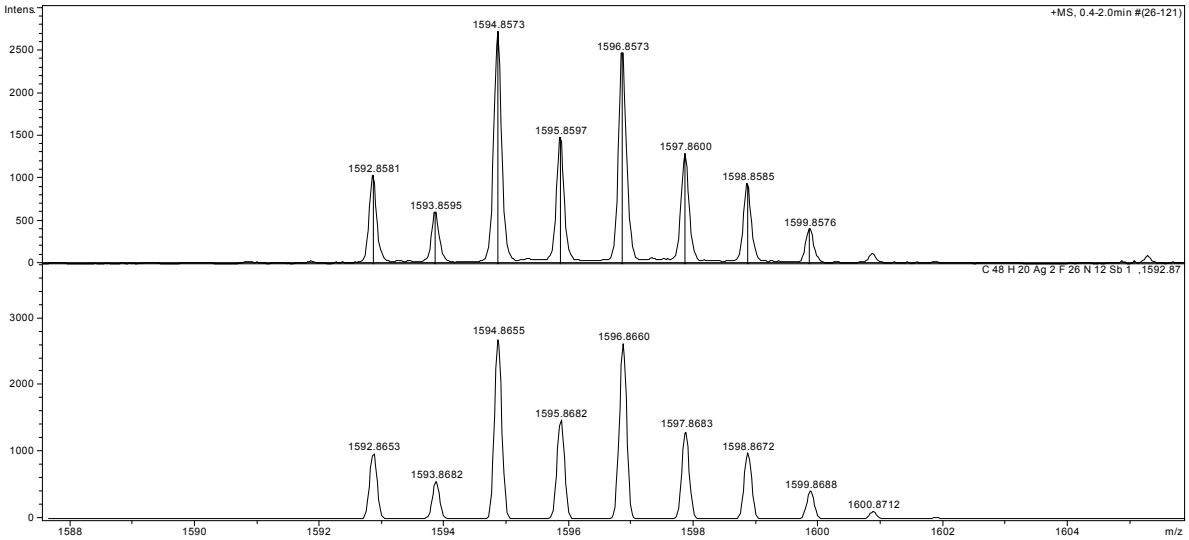

Figure 14. Observed (top) and calculated (bottom) isotopic distribution for the $[Ag_2(\mathbf{3b})_2](SbF_6)^+$ ion.

7. X-ray data for the silver (I) complexes.

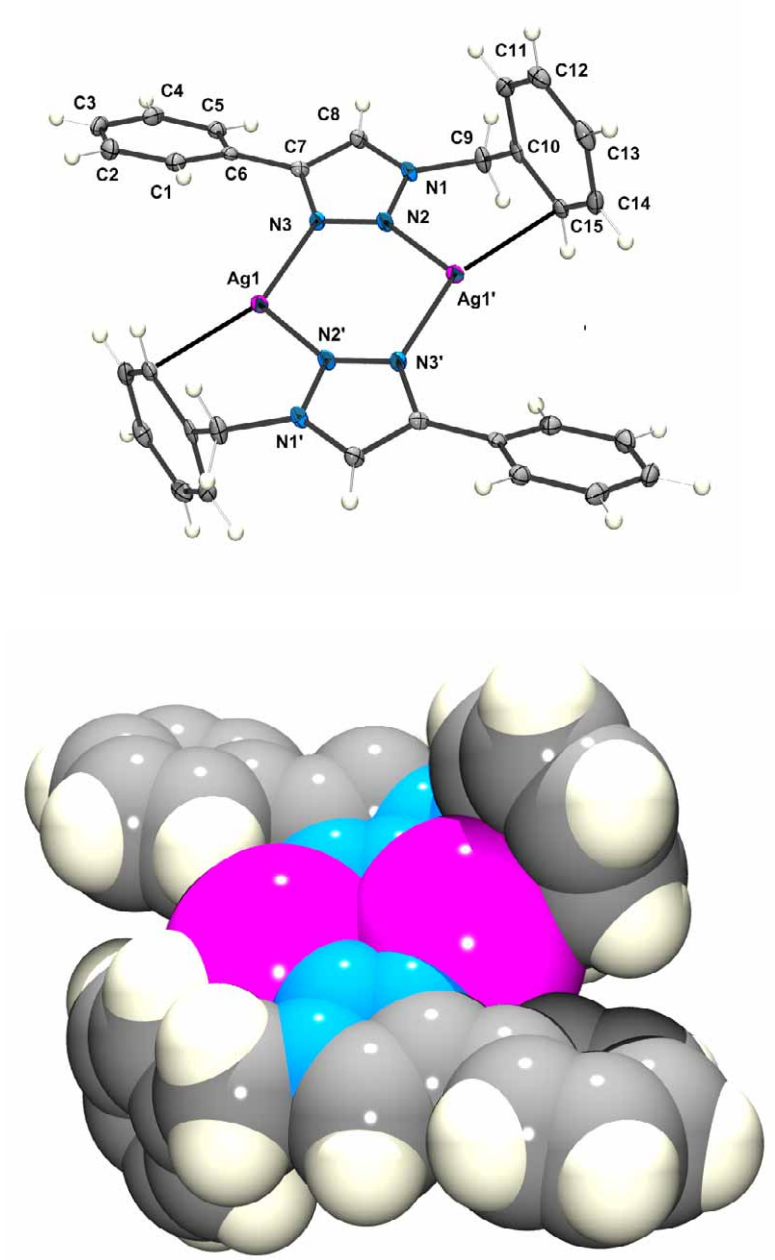

Figure 15. ORTEP (top) and space filling (bottom) views of the $[(\mathbf{2a})_2Ag_2]^{2+}$ cation. The SbF_6^- anions are omitted for clarity.

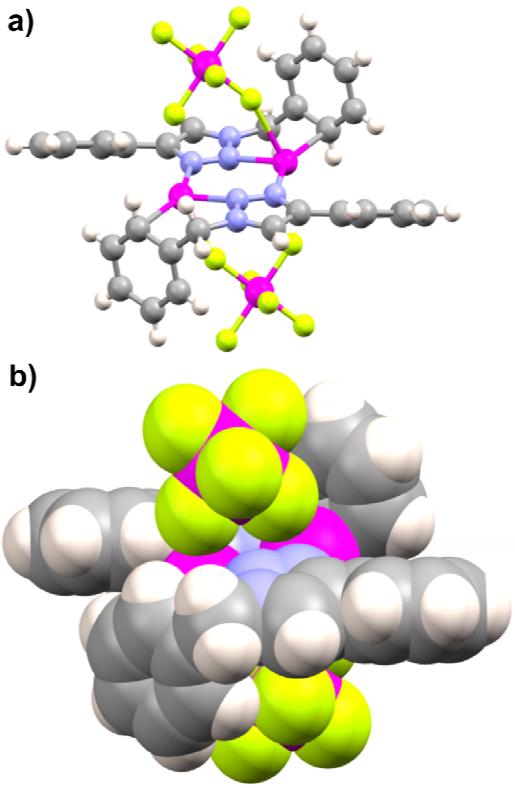

Figure 16. Two views of $[(\mathbf{2a})_2Ag_2](SbF_6)_2$ (**3a**) showing the close contacts between the SbF_6^- anions and the Ag(I) ions. a) a ball and stick diagram and b) a space filing diagram.

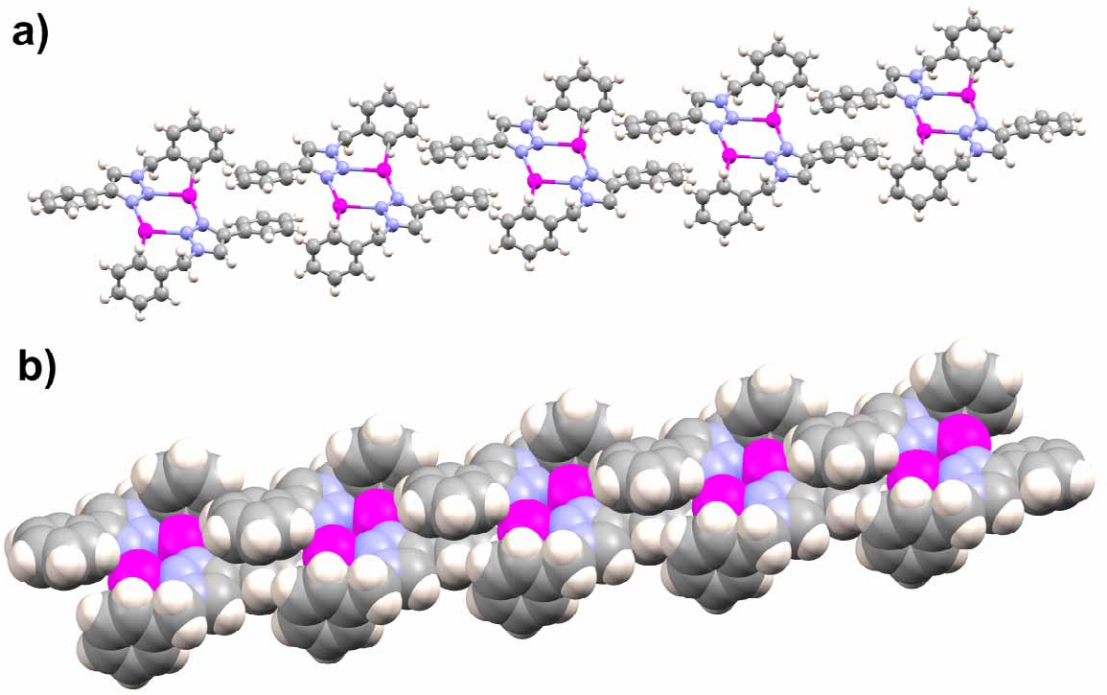

Figure 17. Two views of the extended structure of $[(\mathbf{2a})_2Ag_2](SbF_6)_2$ (**3a**). a) a ball and stick diagram and b) a space filing diagram. The SbF_6^- anions are omitted for clarity.

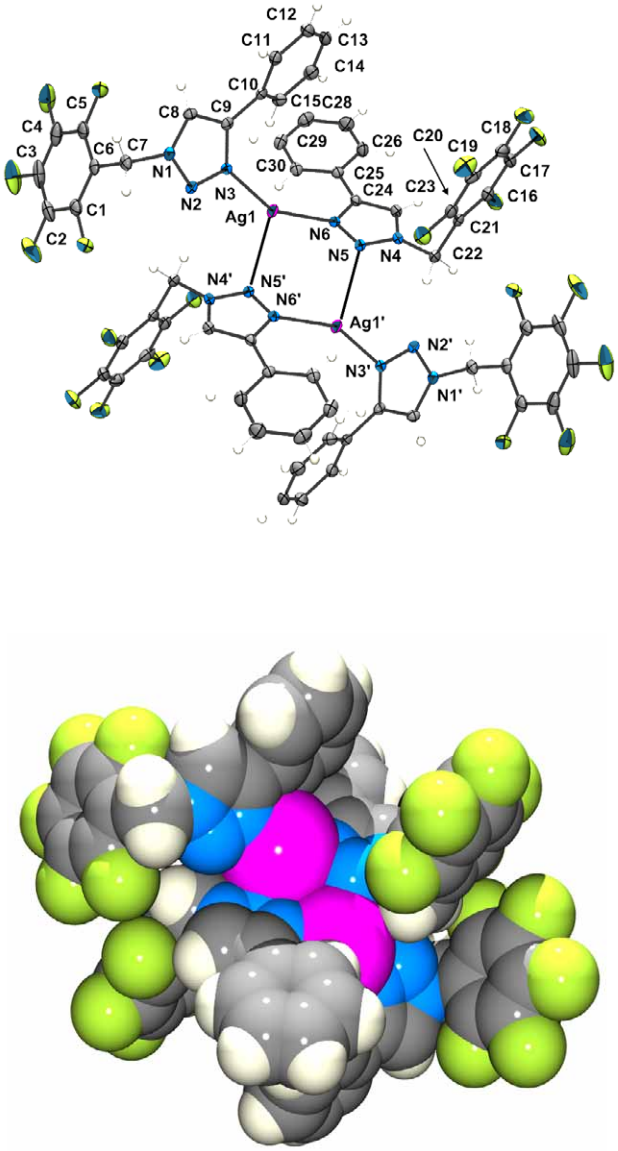

Figure 18. ORTEP (top) and space filling (bottom) views of the $[(\mathbf{2b})_4Ag_2]^{2+}$ cation. The SbF_6^- anions are omitted for clarity.

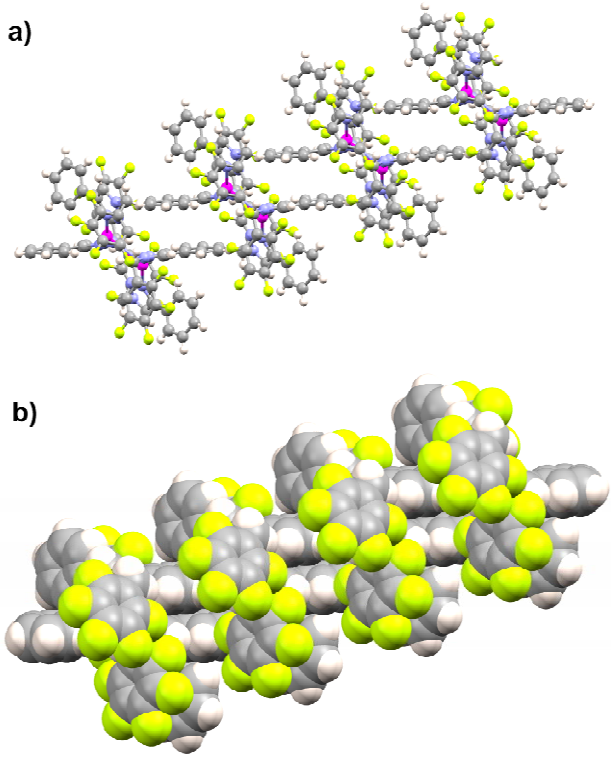

Figure 19. Two views of the extended structure of $[(\mathbf{2b})_2Ag_2](SbF_6)_2$ (**3b**). a) a ball and stick diagram and b) a space filing diagram. The SbF_6^- anions are omitted for clarity.

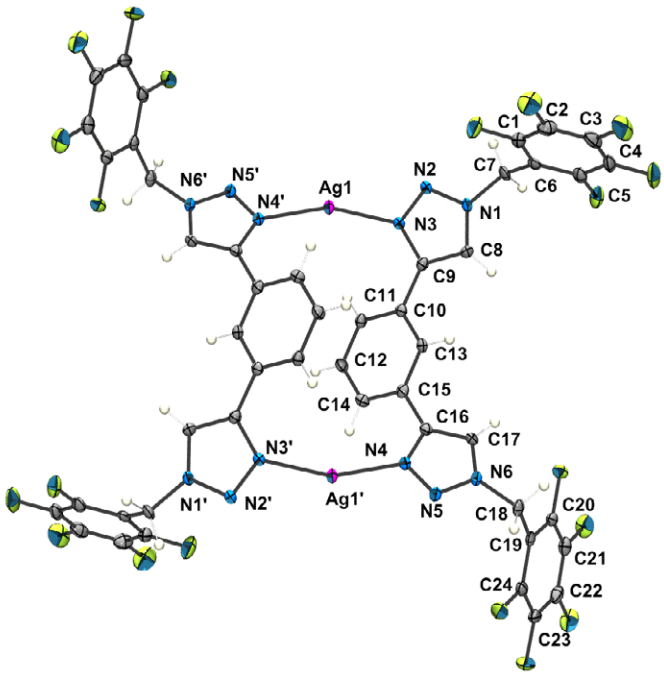

Figure 20. An ORTEP diagram of the $[(\mathbf{3b})_4Ag_2]^{2+}$ cation. The SbF_6^- anions and Et_2O ligands have been omitted for clarity.

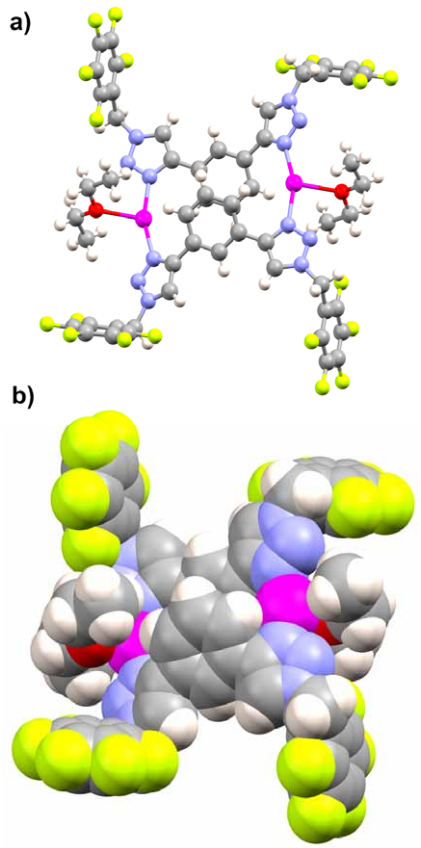

Figure 21. Two views of the complete cationic unit of $[(\mathbf{3b})_2Ag_2](SbF_6)_2$ (**5b**). a) a ball and stick diagram and b) a space filing diagram. The SbF_6^- anions are omitted for clarity.

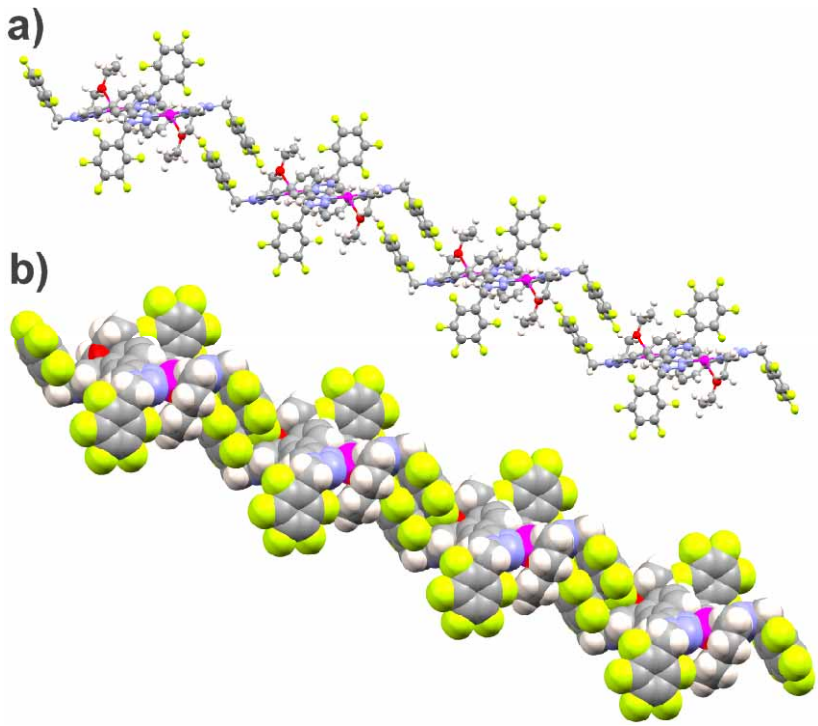

Figure 22. Two views of the extended structure of $[(\mathbf{3b})_2Ag_2](SbF_6)_2$ (**5b**). a) a ball and stick diagram and b) a space filing diagram. The SbF_6^- anions are omitted for clarity.

4.1 X-Ray data collection and refinement for 5b (acetone).

X-Ray data for **5b** (acetone) was recorded with a Bruker APEX II CCD diffractometer at 89(2) K using Mo Kα radiation (λ = 0.71073 Å). The structure was solved by direct methods using SIR97,[1] with the resulting Fourier maps revealing the location of all non-hydrogen atoms of the core metallomacrocycle unit. Following the location of the core atoms of **5b** (acetone) in the ΔF map there was still residual electron density present near the silver atoms of the structure. This was modelled as coordinated acetone. However, these acetone molecules are badly disordered. Disappointingly, this disorder could not be satisfactorily resolved; as such there is residual electron density around the coordinated acetone molecules within the structure. One of the pentafluorobenzyl groups displayed large thermal parameters potentially due to further disorder, as such it was restrained using ISOR and SIMU commands in SHELXL-97[2]. Weighted full matrix refinement on F^2 was carried out using SHELXL-97[2] with all non-hydrogen atoms being refined anisotropically, while the disordered acetone molecules were refined isotropically. The hydrogen atoms were included in calculated positions and were refined as riding atoms with individual (or group, if appropriate) isotropic displacement parameters.

The ORTEP[3] diagrams have been drawn with 50% probability ellipsoids. Crystal data and collection parameters are given in Table 1.

Table 1 Crystal data and structure refinement for **5b** (acetone)**.**

Identification code	**5b** (acetone) CCDC 751439
Empirical formula	$C_{33}H_{28}O_3F_{16}AgSbN_6$
Formula weight	1090.23
Temperature	89(2)
Crystal system	Monoclinic
Space group	$P2_1/n$
a/Å, b/Å, c/Å	19.902(4), 9.080(2), 23.168(5)
α/°, β/°, γ/°,	90, 113.594(1), 90
Volume/Å^3	3836.7(14)
Z	4
ρ_{calc}mg/mm^3	1.887

m/mm^{-1}	1.336
F(000)	2136
Crystal size	0.58 × 0.28 × 0.07
Theta range for data collection	1.14 to 24.59°
Index ranges	$-23 \leq h \leq 23$, $-10 \leq k \leq 10$, $-27 \leq l \leq 27$
Reflections collected	72868
Independent reflections	6446 [R(int) = 0.062]
Data/restraints/parameters	6446/127/503
Goodness-of-fit on F^2	1.078
Final R indexes [I>2σ (I)]	$R_1 = 0.0801$, $wR_2 = 0.206$
Final R indexes [all data]	$R_1 = 0.0873$, $wR_2 = 0.2119$
Largest diff. peak/hole	3.089/-1.063

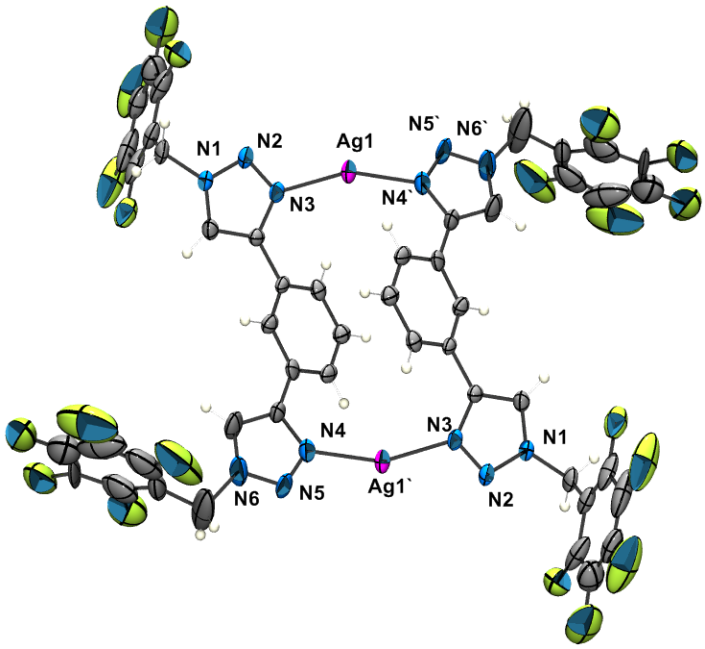

Figure 23. An ORTEP diagram of $[(\mathbf{3b})_4Ag_2]^{2+}$ cation from the of the crystal structure **5b** (acetone). The SbF_6^- anions and acetone ligands have been omitted for clarity.

5. References

1. A. Altomare, M. C. Burla, M. Camalli, G. L. Cascarano, C. Giacovazzo, A. Guagliardi, A. G. G. Moliterni, G. Polidori and R. Spagna, *J. Appl. Crystallogr.*, 1999, **32**, 115-119.
2. G. M. Sheldrick, *Acta Crystallogr., Sect. A: Found. Crystallogr.*, 2008, **A64**, 112-122.
3. L. J. Farrugia, *J. Appl. Crystallogr.*, 1997, **30**, 565.